Processes underlying the laser photochromic effect in colloidal plasmonic nanoparticle aggregates*

A E Ershov[1,2,†], V S Gerasimov [1,2], I L Isaev [1], A P Gavrilyuk[1,2], and S V Karpov[2,3,4]

[1] *Institute of Computational Modeling SB RAS, 660036, Krasnoyarsk, Russia*
[2] *Siberian Federal University, Krasnoyarsk, 660041, Russia*
[3] *Kirensky Institute of Physics, Federal Research Center KSC SB RAS, 660036, Krasnoyarsk, Russia*
[4] *Siberian State University of Science and Technology, Krasnoyarsk 660014, Russia*

(Received 19 September 2019; revised manuscript received 12 December 2019; accepted manuscript online 24 December 2019)

We have studied the dynamic and static processes occurring in disordered multiparticle colloidal Ag aggregates with natural structure and affecting their plasmonic absorption spectra under pico- and nanosecond pulsed laser radiations, as well as the physical origin responsible for these processes. We have shown that depending on the duration of the laser pulse, the mechanisms of laser modification of such aggregates can be associated both with changes in the resonant properties of the particles due to their heating and melting (picosecond irradiation mode) and with the particle shifts in the resonant domains of the aggregates (nanosecond pulses) which depend on the wavelength, intensity, and polarization of the radiation. These mechanisms result in formation of a narrow dip in the plasmonic absorption spectrum of the aggregates near the laser radiation wavelength and affect the shape and position of the dip. The effect of polydispersity of nanoparticle aggregates on laser photochromic reaction has been studied.

Keywords: nanoparticle, surface plasmon resonance, photochromic process, pulsed laser radiation

PACS: 78.67.Sc, 73.20.Mf **DOI:** 10.1088/1674-1056/ab6551

1. Introduction

Nanosized plasmonic structures are widely employed as modificators of the optical properties of various optically sensitive objects and materials, such as molecules and their aggregates. The modification effect is demonstrated in giant enhancement of Raman sensing, the efficiency of solar cells, fluorescence, nonlinear optical phenomena, and so on. Experimental studies have brought many interesting results and have been supported both by theoretical and computational researches.[1–8] The physics of the interaction of pulsed laser radiation with aggregates of plasmonic nanoparticles and impurity materials located in the vicinity of such nanostructures covers a wide range of research and applied problems.[9–15] However, on the way of obtaining the physical insight into the nature of field enhancement and prediction of the best nanostructured intermediary media (such as plasmonic nanoparticles and their aggregates) in high intensity pulsed laser fields, we encounter with the problem of variation of the properties of the intermediary media responsible for the enhancement field effect. On the one hand, it worsens this enhancement, but on the other hand, it demonstrates the effect of the optical memory of such media at the given wavelength that is of particular interest.

Colloidal aggregates of classical plasmonic materials (Ag or Au) with a locally anisotropic structure[16,17] are able to enhance the spatially localized electromagnetic fields near the plasmonic nanoparticles resonant to the incident optical radiation and this enhancement is observed in the range of an inhomogeneously broadened plasmonic absorption band.[18] In a simplified form, the large aggregates can be considered as a set of resonant domains, i.e., small groups of closely spaced nanoparticles in an aggregate, characterized by their eigen frequencies resonant to the incident radiation with a spectral width corresponding to the surface plasmon absorption band of the individual particles.

Despite the large volume of experimental data in such materials and sustainable reproducibility of the effects in pulsed laser radiation, the observed phenomena have not received due explanation because of the complexity and interconnection of related processes.

This photochromic effect in aggregated plasmonic nanocolloids was first discovered in Ref. [19] and was studied in more detail experimentally in later works.[20,21] This effect clearly reveals itself in the case when the pulsed laser radiation frequency lies within the plasmonic absorption band of the disordered aggregates and when the energy threshold is exceeded. Under this condition, the irradiated area acquires transparency at the laser radiation wavelength corresponding to the color of radiation. The absorption spectrum of the nanoparticle aggregate acquires a spectral dip with a width corresponding to

*Project funded by the Russian Foundation for Basic Research, the Government of the Krasnoyarsk Territory and Krasnoyarsk Regional Fund of Science (Grant 18-42-243023), the RF Ministry of Science and Higher Education, and the State Contract with Siberian Federal University for Scientific Research. A.E. thanks the grant of the President of Russian Federation (agreement 075-15-2019-676).

†Corresponding author. E-mail: aleksander.ershow@yahoo.com

the plasmonic absorption spectrum of an individual particle. Herewith, the shape of the spectral dip determines the features of nonlinear refraction of such media.

Among the unsolved problems we should note the lack of complete understanding of the dominant mechanisms of modification of optical properties of plasmonic nanocolloids. In particular, it was found that one of the mechanisms of optical nonlinearity[22,23] of aggregated plasmonic nanocolloids and nanocomposites is the effect of the radiation induced transparency under the influence of laser pulses. Herewith, this effect demonstrates the spectral and polarization selectivity.

In Refs. [6,7,24], the models of the interaction of pulsed laser radiation with multiparticle plasmonic aggregates of spherical metal nanoparticles have been first developed. Reference [7] presented the modified optodynamic model that takes into account the polydispersity of the nanoparticles and their interactions, dissipation of absorbed energy, heating and melting of the metal core and polymer adsorption layer of the particle, heat exchange between the electron and lattice components of the metal, as well as with the interparticle medium. Optical interparticle interactions were taken into account via the dipole–dipole nanoparticle interactions. The dipole moment of each particle was calculated by the coupled dipole method.[25] To take into account the contribution of higher multipoles, we used the rescaled parameter according to the method described in Refs. [7,26]. In Refs. [7,27], the role and contribution of various interrelated factors resulting in the laser modification of simple resonant domains such as dimers and trimers in picosecond laser pulses have been studied.

It was shown that the evolution of the spectral properties of a resonance domain dynamically varying resonant frequency during the laser pulse can be associated with changes in the size, shape, and state of material of the particles, and after the pulse end, with a shift of neighboring particles in a domain relative to each other. Such processes in pulsed laser fields result in the modification of the resonant domains and large colloidal aggregates which cause photochromic reactions in nanocolloids and nanocomposite materials.

The goal of our paper is to study the dynamic processes occurring in disordered multiparticle polydisperse colloidal aggregates with realistic structure and affecting their plasmonic extinction spectra under the pulsed pico- and nanosecond laser radiation, as well as the physical mechanisms responsible for these processes during the laser radiation.

Compared to our previous papers studying these processes in dimers and trimers, we investigate the processes in sets of 2000 large aggregates composed of 50-particle with subsequent averaging over a set. Limitation of the number of particles to 50 instead of 1000 and more makes it possible to shorten significantly the computation time. Besides that, we have compared these effects in monodisperse and polydisperse aggregates (Fig. 1).

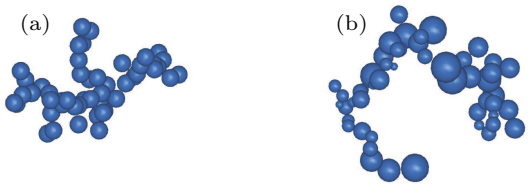

Fig. 1. Examples of (a) monodisperse and (b) polydisperse nanoparticle aggregates consisting of 50 Ag polymer coated nanoparticles used in calculations.

2. Model

The photochromic mechanisms are based on the analytical model of interaction of high intensity laser radiation with multiparticle aggregate of plasmonic nanoparticles. The developed optodynamic model of the interaction of multiparticle aggregates with pulsed laser radiation takes into account a wide range of interrelated thermodynamic, optical, physicochemical, and mechanical processes. Our model takes into account the results from Refs. [28–31], in particular, with discussion on the possibilities of the light-induced shift of particles in aggregates and nonlinear optical effects caused by this shift, as well as the effect of different sizes of particles on their interaction in optical fields.[32] In our work we present the most complete model taking into account in previous publications.

In our model, we solve the following ordinary differential equation system which describes the motion of each particle in an aggregate:

$$\frac{\mathrm{d}\boldsymbol{r}_i}{\mathrm{d}t} = \boldsymbol{v}_i, \quad i = 1,\ldots,N, \tag{1}$$

$$m_i \frac{\mathrm{d}\boldsymbol{v}_i}{\mathrm{d}t} = (\boldsymbol{F}_{\mathrm{vdw}})_i + (\boldsymbol{F}_{\mathrm{el}})_i + (\boldsymbol{F}_{\mathrm{opt}})_i + (\boldsymbol{F}_{\mathrm{v}})_i + (\boldsymbol{F}_{\mathrm{f}})_i. \tag{2}$$

Here t is the time from the onset of the pulse; m_i, R_i, $\boldsymbol{v}_i$, and $\boldsymbol{r}_i$ are the mass, radius, speed, and radius vector of the center of mass of the i-th particle; and N is the number of particles in an aggregate.

The right side of Eq. (2) is the sum of the forces acting on the particle

$$\begin{aligned}
(\boldsymbol{F}_{\mathrm{vdw}})_i &= -\sum_{\substack{j=1\\ j\neq i}}^{N} \frac{\partial (U_{\mathrm{vdw}})_{ij}}{\partial \boldsymbol{r}_i}, \\
(\boldsymbol{F}_{\mathrm{el}})_i &= -\sum_{\substack{j=1\\ j\neq i}}^{N} \frac{\partial (U_{\mathrm{el}})_{ij}}{\partial \boldsymbol{r}_i}, \\
(\boldsymbol{F}_{\mathrm{opt}})_i &= -\frac{\partial U_{\mathrm{opt}}}{\partial \boldsymbol{r}_i}, \\
(\boldsymbol{F}_{\mathrm{v}})_i &= -6\pi\eta(R_i + h_i)\boldsymbol{v}_i, \\
(\boldsymbol{F}_{\mathrm{f}})_i &= -\mu \sum_{\substack{j=1\\ j\neq i}}^{N} \left|(\boldsymbol{F}_{\mathrm{el}})_{ij}\right| \boldsymbol{q}_{ij}.
\end{aligned} \tag{3}$$

Here $(\boldsymbol{F}_{\rm vdw})_i$ is the van der Waals attractive force; $(\boldsymbol{F}_{\rm el})_i$ is the elastic repulsive force related to deformation of the adlayers of contacting particles;[33] $(\boldsymbol{F}_{\rm opt})_i$ is the optical force caused by the interaction of the light-induced dipoles; $(\boldsymbol{F}_{\rm v})_i$ is the viscous friction force; $(\boldsymbol{F}_{\rm f})_i$ is the tangential interparticle friction forces; η is the dynamical viscosity of the interparticle medium; h_i is the thicknesses of undeformed particle's adsorption layer; μ is the effective friction coefficient, and $\boldsymbol{q}_{ij}$ is the normalized vector of the projection of the particles relative velocity on the plane of contact of particle adlayers

$$\boldsymbol{q}_{ij}=\frac{(\boldsymbol{v}_j-\boldsymbol{v}_i)-\boldsymbol{n}_{ij}((\boldsymbol{v}_j-\boldsymbol{v}_i)\cdot\boldsymbol{n}_{ij})}{\left|(\boldsymbol{v}_j-\boldsymbol{v}_i)-\boldsymbol{n}_{ij}((\boldsymbol{v}_j-\boldsymbol{v}_i)\cdot\boldsymbol{n}_{ij})\right|},$$

with $\boldsymbol{n}_{ij}=\boldsymbol{r}_{ij}/|\boldsymbol{r}_{ij}|$, and $\boldsymbol{r}_{ij}=\boldsymbol{r}_i-\boldsymbol{r}_j$ being the vector connecting the centers of the particles.

For conservative forces in Eq. (3), we can write the potential energy equations

$$\begin{aligned}(U_{\rm vdw})_{ij} &= -\frac{A_{\rm H}}{6}\left(\frac{2R_iR_j}{h_{ij}^2+2R_ih_{ij}+2R_jh_{ij}}\right.\\&\quad+\frac{2R_iR_j}{h_{ij}^2+2R_ih_{ij}+2R_jh_{ij}+4R_iR_j}\\&\quad\left.+\ln\frac{h_{ij}^2+2R_ih_{ij}+2R_jh_{ij}}{h_{ij}^2+2R_ih_{ij}+2R_jh_{ij}+4R_iR_j}\right),\end{aligned}\tag{4}$$

$$\begin{aligned}(U_{\rm el})_{ij} &= \frac{8}{15}(h_i+h_j-h_{ij})^{5/2}\left[\frac{(R_i+h_i)(R_j+h_j)}{R_i+h_i+R_j+h_j}\right]^{1/2}\\&\quad\times\frac{(E_{\rm el})_i\cdot(E_{\rm el})_j}{(E_{\rm el})_i+(E_{\rm el})_j}H(h_i+h_j-h_{ij}),\end{aligned}\tag{5}$$

$$\begin{aligned}U_{\rm opt} &= -\frac{1}{4}{\rm Re}\sum_{i=1}^{N}\left[\boldsymbol{d}_i\cdot\boldsymbol{E}^*(\boldsymbol{r}_i)+\frac{1}{2}\boldsymbol{d}_i\cdot\left(\frac{\boldsymbol{d}_i}{\varepsilon_0\alpha_i}-\boldsymbol{E}(\boldsymbol{r}_i)\right)^*\right.\\&\quad\left.-\varepsilon_0\alpha_i|\boldsymbol{E}_0|^2\right]\cdot H(\tau-t).\end{aligned}\tag{6}$$

Here $(U_{\rm vdw})_{ij}$ is the energy of the van der Waals interaction between the i-th and j-th particles;[34] $(U_{\rm el})_{ij}$ is the energy of elastic interaction between two adsorption layers; $U_{\rm opt}$ is the energy of interaction of light-induced dipoles; $A_{\rm H}$ is the Hamaker constant for silver;[35] $h_{ij}=|\boldsymbol{r}_{ij}|-(R_i+R_j)$ is the interparticle gap; $(E_{\rm el})_i$, $(E_{\rm el})_j$ are the elasticity moduli of the particle adlayers; $H(x)$ is the Heaviside function; $\boldsymbol{d}_i$ is the light-induced dipole moment; $\boldsymbol{E}(\boldsymbol{r})$ is the strength of the external electromagnetic field, $\boldsymbol{E}_0$ is the amplitude of the field, the symbol $*$ denotes the complex conjugation; α_i is the dipole polarizability of the i-th particle; and τ is the laser pulse duration.

The coupled dipoles method is used to calculate the dipole moments of particles and spectra of multi-particle aggregates[25] (in SI):

$$d_{i\alpha}=\varepsilon_0\alpha_i\left[E_\alpha(\boldsymbol{r}_i)+\sum_{\substack{j=1\\j\neq i}}^{N}\sum_{\beta=1}^{3}G_{\alpha\beta}(\boldsymbol{r}'_{ij})d_{j\beta}\right],\tag{7}$$

$$\begin{aligned}&\boldsymbol{E}(\boldsymbol{r})=\boldsymbol{E}_0\exp({\rm i}\boldsymbol{k}\cdot\boldsymbol{r}),\\&G_{\alpha\beta}(\boldsymbol{r})=\frac{|\boldsymbol{k}|^3}{\varepsilon_0}\left(A(|\boldsymbol{k}||\boldsymbol{r}|)\delta_{\alpha\beta}+B(|\boldsymbol{k}||\boldsymbol{r}|)\frac{r_\alpha r_\beta}{|\boldsymbol{r}|^2}\right),\\&A(x)=\left(x^{-1}+{\rm i}x^{-2}-x^{-3}\right)\exp({\rm i}x),\\&B(x)=\left(-x^{-1}-3{\rm i}x^{-2}+3x^{-3}\right)\exp({\rm i}x),\\&\sigma_{\rm e}=\frac{4\pi|\boldsymbol{k}|}{\varepsilon_0}{\rm Im}\left(\sum_{i=1}^{N}\frac{\boldsymbol{d}_i\cdot\boldsymbol{E}^*(\boldsymbol{r}_i)}{|\boldsymbol{E}_0|^2}\right),\quad Q_{\rm e}=\frac{\sigma_{\rm e}}{\sum\limits_{i=1}^{N}\pi R_i^2}.\end{aligned}\tag{8}$$

Here $\boldsymbol{k}$ is the wave vector of the laser radiation; α_i is the dipole polarizability of the i-th particle; $\boldsymbol{r}'_{ij}$ is the vector connecting the centers of the particles, adjusted by the rescaling parameter[7,26] ξ:

$$\boldsymbol{r}'_{ij}=\begin{cases}\boldsymbol{r}_{ij}/\xi, & \text{if}\quad r_{ij}\leq 1.5(R_i+R_j),\\ \boldsymbol{r}_{ij}, & \text{if}\quad |\boldsymbol{r}_{ij}|>1.5(R_i+R_j),\end{cases}$$

$G_{\alpha\beta}$ is the interparticle interaction tensor; $\delta_{\alpha\beta}$ is the Kronecker delta; ε_0 is the electric constant; $\sigma_{\rm e}$ is the extinction cross section, $Q_{\rm e}$ is the extinction efficiency, and Greek subscripts denote the Cartesian components of the vectors and tensors.

The dipole polarizability of a particle taking into account self-action reads as[25]

$$\alpha_i=R_i^3\frac{\varepsilon_i-\varepsilon_{\rm m}}{\varepsilon_i+2\varepsilon_{\rm m}-\frac{2}{3}{\rm i}(R_i\omega/c)^3(\varepsilon_i-\varepsilon_{\rm m})},\tag{9}$$

where ω is the angular frequency of the laser radiation, c is the speed of light in vacuum, $\varepsilon_{\rm m}$ is the dielectric constant of the interparticle medium; ε_i is the dielectric constant of the particle taking into consideration its size, temperature, and state of matter.

The dependence of ε_i on the aggregate state of the metal (taking into account that a particle can contain both a liquid and a solid phase at some time interval) is described by the following equation:

$$\varepsilon_i=f_i\varepsilon_i^{\rm (L)}+(1-f_i)\varepsilon_i^{\rm (S)},$$

where $\varepsilon_i^{\rm (S)}$ and $\varepsilon_i^{\rm (L)}$ are the dielectric constants of the solid and liquid phases of the particle, and f_i is the mass fraction of the liquid in the particle

$$f_i=\begin{cases}0, & \text{if}\quad (Q_{\rm i})_i<(Q_1)_i,\\ 1, & \text{if}\quad (Q_{\rm i})_i>(Q_2)_i,\\ \dfrac{(Q_{\rm i})_i-(Q_1)_i}{(Q_2)_i-(Q_1)_i}, & \text{otherwise},\end{cases}$$

with $(Q_{\rm i})_i$ being the thermal energy transferred to the ion component of the particle, $(Q_1)_i$ and $(Q_2)_i$ the thermal energies at the initial and final stages of melting (see the equations below).

The dependence of the dielectric constant of the phase state (solid (S) or liquid (L)) is described by the equation[8]

$$\varepsilon_i^{\rm (S,L)}=\varepsilon_{\rm int}(\omega)-\frac{\omega_{\rm p}^2}{\omega^2+{\rm i}\omega\Gamma^{\rm (S,L)}((T_{\rm i})_i,R_i)}.\tag{10}$$

Here $\varepsilon_{\text{int}}(\omega)$ is the factor that takes into account the contribution of interband transitions to the dielectric constant, ω_{p} is the plasma frequency of the metal, $\Gamma^{(\text{S,L})}(T,R)$ is the relaxation constant of the electron subsystem for the solid or liquid phase (taking into account the size of the particle and the finite size effect)

$$\Gamma^{(\text{S,L})}(T,R) = \Gamma_{\infty}^{(\text{S,L})}(T) + \kappa\frac{v_{\text{F}}}{R}, \tag{11}$$

where v_{F} is the Fermi velocity, κ is the constant assumed to be equal to 1 in most of the optical calculations,[36] $\Gamma_{\infty}^{(\text{S,L})}(T)$ is the relaxation constant corresponding to the frequency of scattering of conduction electrons at phonons and lattice defects. The dependence of $\Gamma_{\infty}^{(\text{S,L})}$ on temperature is assumed to be linear,[8]

$$\Gamma_{\infty}^{(\text{S,L})}(T) = C_1^{(\text{S,L})}T + C_2^{(\text{S,L})}. \tag{12}$$

Here $C_1^{(\text{S,L})}$ and $C_2^{(\text{S,L})}$ are constants, obtained from experimental data for solid ($C_1^{(\text{S})}$, $C_2^{(\text{S})}$) and liquid ($C_1^{(\text{L})}$, $C_2^{(\text{L})}$) fractions.[8]

The model takes into account the heating of the particle material by optical radiation using the two-component model, which takes into account separately the temperatures of the electron and ion subsystems of the particle material. The change in the electron temperature occurs due to the absorption of optical energy by the particle, as well as due to heat exchange with the ionic component

$$(C_{\text{e}})_i\frac{\text{d}(T_{\text{e}})_i}{\text{d}t} = -g\left[(T_{\text{e}})_i - (T_{\text{i}})_i\right] + \frac{W_i}{V_i}, \tag{13}$$

where $(T_{\text{e}})_i$ and $(T_{\text{i}})_i$ are the temperatures of the electron and lattice (ion) components of the i-th particle; $(C_{\text{e}})_i$ is the volumetric heat capacity of the electron component; g is the rate of energy exchange between the electron and ion subsystems; $V_i = 4/3\pi R_i^3$ is the particle volume; W_i is the absorbed power of laser radiation:

$$W_i = \frac{\omega|\boldsymbol{d}_i|^2}{2\varepsilon_0}\text{Im}\left(\frac{1}{\alpha_i^*}\right).$$

Taking into account that a phase transition (melting/crystallization) occurs in the particle material, the thermodynamics of the ionic component is described in terms of the amount of heat $(Q_{\text{i}})_i$ transferred to the ionic component. The model takes into account the heat exchange with the electron component and the environment

$$\frac{\text{d}(Q_{\text{i}})_i}{\text{d}t} = gV_i\left[(T_{\text{e}})_i - (T_{\text{i}})_i\right] + (q_{\text{l}})_iV_i, \tag{14}$$

where $(q_{\text{l}})_i$ is the heat flow per unit volume describing thermal losses[37]

$$(q_{\text{l}})_i = -\frac{3}{2R_i}(\chi_{\text{m}}c_{\text{m0}}\rho_{\text{m}})^{1/2}\cdot\left[(T_{\text{i}})_i - T_0\right]\cdot t^{-1/2}. \tag{15}$$

Here χ_{m} is the thermal conductivity of the interparticle medium, c_{m0} is its heat capacity, ρ_{m} is the density, t is the time since the beginning of a pulse, and T_0 is the temperature of the interparticle medium.

The temperature of the ionic component is described in terms of the amount of heat as follows:

$$(T_{\text{i}})_i = \begin{cases} \dfrac{(Q_{\text{i}})_i}{C_iV_i}, & \text{if} \quad (Q_{\text{i}})_i < (Q_1)_i, \\ \dfrac{(Q_{\text{i}})_i - ((Q_2)_i - (Q_1)_i)}{C_iV_i}, & \text{if} \quad (Q_{\text{i}})_i > (Q_2)_i, \\ T_{\text{m}}(R_i), & \text{otherwise}, \end{cases}$$

where $T_{\text{m}}(R_i)$ is the size dependence of the melting temperature.

The model takes into account the change in the elasticity modulus of the particle absorption layers, which is associated with the heating and destruction of molecular bonds in the absorption layer of nanoparticles. This happens within a finite relaxation time τ_{r}, which can be described by the equation[6]

$$\tau_{\text{r}}(T) = \tau_0\exp\left(\frac{U}{k_{\text{B}}T}\right),$$

where the value of τ_0 is assumed to be 10^{-12} s, U is the energy of chemical bonds in the polymer adlayer (taken to be about 1 eV in our calculations, which is typical of the chemical bond energy of polymers).[7]

Taking into account the finite relaxation time, the dependence on temperature of the elasticity modulus of the absorption layer is described by the following equation:[6]

$$\frac{\text{d}(E_{\text{el}})_i}{\text{d}t} = -\frac{(E_{\text{el}})_i}{\tau_{\text{r}}((T_{\text{m}})_i)}, \tag{16}$$

where $(T_{\text{m}})_i = ((T_{\text{i}})_i - T_0)/2$ is the average temperature of the heated area near the i-th particle.

The numerical implementation is the solution of the ordinary differential equation system (1), (2), (11), (12), (16) with respect to the parameters $\boldsymbol{r}_i$, $\boldsymbol{v}_i$, $\boldsymbol{v}_i$, $(T_{\text{e}})_i$, $(Q_{\text{i}})_i$, $(E_{\text{el}})_i$ taking into account the fact that the right-hand side depends on the values of $\boldsymbol{d}_i$ which are the solutions of the system of linear algebraic equation (7). This solution provides the optical and thermodynamic characteristics of domains and their kinetics.

3. Results

In this section, we present the results of calculations of the photomodification of Ag multiparticle disordered aggregates with a locally anisotropic structure under the action of short laser pulses of high intensity. To perform the calculations, we used a set of 2000 aggregates generated with the method of Brownian dynamics,[38] which reproduced the structure of natural colloidal aggregates. The extinction spectra of such aggregates were averaged over this set.

3.1. Picosecond laser pulses

The feature of picosecond laser irradiation is that, due to the inertia of nanoparticles they do not have time during the short laser pulse to change their position in the resonance domains under the action of the van der Waals forces in conditions of a decrease in the elasticity modulus of the adsorption layer of the particles as well as under the influence of the optical interaction.[7] In such time scales, changes in extinction spectra are caused exclusively by variations in the resonant properties of the particles in the domains as a result of their heating and melting.

Figure 2 shows the extinction spectra of monodisperse and polydisperse aggregates consisting of 50 Ag nanoparticles, with 5 nm radius for the monodisperse aggregates and with radii from 2 nm to 8 nm, distributed over the truncated Poisson function for the polydisperse aggregates. In order to take into account in the calculations the contribution of multipole modes, we used the intersection coefficient,[11] the value of which was determined by correspondence of the long-wavelength wing of the extinction spectrum to the experimental ones. We can see that the polydisperse aggregates have a greater broadening in the long-wavelength wing of the spectrum.[26]

Figure 3 shows the difference spectra of polydisperse and monodisperse aggregates. The spectra are averaged over 2000 aggregates and over three mutually perpendicular polarizations of the incident laser radiation. The dependences show the effect of the pulsed laser radiation on the disordered aggregates of Ag nanoparticles which is accompanied by the formation of a spectrally selective dip near the laser wavelength. The depth of the spectral dip in the case of polydisperse aggregates exceeds that for monodisperse aggregates, while the difference in the depth of the dip increases for larger radiation wavelength. This is due to higher spectral density of resonances in the long-wavelength range for polydisperse aggregates (Fig. 2).

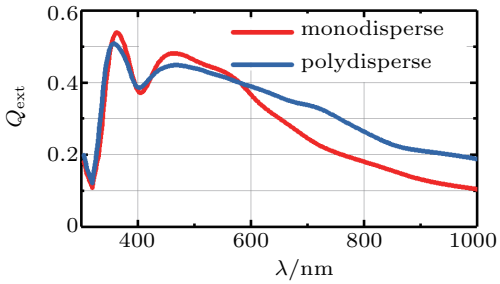

Fig. 2. Extinction spectra of aggregates consisting of 50 nanoparticles with $R = 5$ nm for monodisperse and R in a range from 2 nm to 8 nm for polydisperse aggregates.

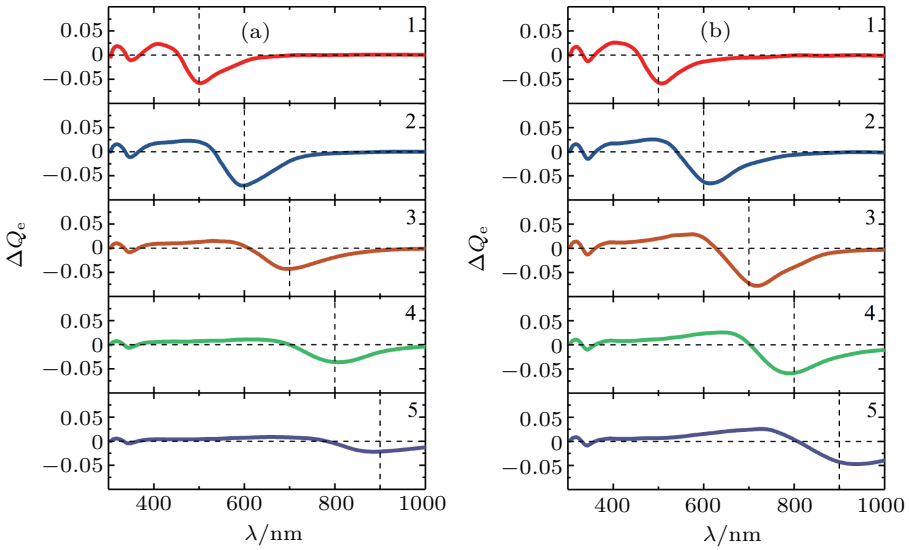

Fig. 3. Differential extinction spectra of (a) multiparticle monodisperse and (b) polydisperse aggregates of Ag nanoparticles at the moment of termination of a laser pulse with a duration of 20 ps and an intensity of 2.4×10^8 W·cm^{-2}, the vertical dotted line indicates the laser wavelength.

Figure 4 shows similar differential spectra obtained at 40 ns after the start of the laser pulse. As the time elapses since the end of the laser pulse, the system comes into a state of mechanical and thermodynamic equilibrium, which can be preserved much longer than the duration of the laser pulse. It can be seen that, due to the melting of the particles, the humps in the short-wave part of the spectrum of polydisperse aggregates disappear over time, which is associated with the cooling and crystallization of small nanoparticles. In turn, the formation of humps in the long-wave range of the spectrum is a result of shift and collapse of particles in resonant domains. This effect does not manifest itself during short time picosecond pulses due to the inertia of the particles.

Note, when Ag colloidal aggregates are irradiated with picosecond laser pulses, a short-wavelength shift in spectral dips may be observed, and likely cause of this shift may be associated with the involvement of short-wave quasi-resonance domains in the laser modification process. We also note that

experimental registration of changes in plasmonic absorption spectra is carried out during much longer time – for several minutes, that may be accompanied by additional restructuring process in the aggregates.

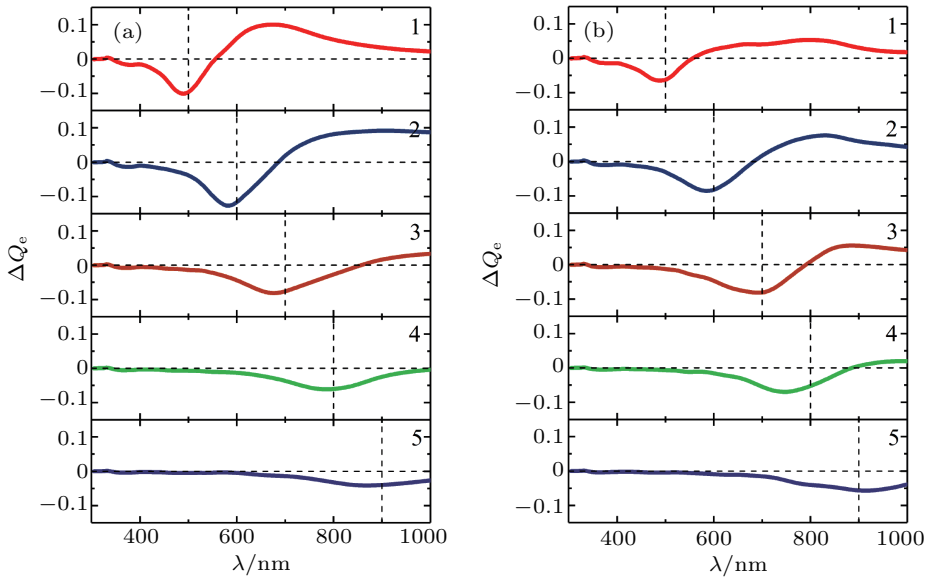

Fig. 4. Differential extinction spectra of (a) monodisperse and (b) polydisperse aggregates of Ag nanoparticles 40 ns later the beginning of a laser pulse of 20 ps duration with the intensity of 2.4×10^8 W· cm^{-2}, the vertical dotted line indicates the laser wavelength.

3.2. Nanosecond pulses

Simulations of the photomodification and its spectral manifestation have been carried out for laser pulses with a duration of 20 ns and the radiation intensity 2.66×10^5 W·cm^{-2} (Figs. 5 and 6). Under these conditions, the other processes can cause the modification of the aggregates.

We can see in Fig. 5 at the pulse end the formation of a dip and the hump adjacent to it in the long-wave range of the differential extinction spectra of both monodisperse and polydisperse aggregates. In this case, their formation is explained by the fact that during the action of a long laser pulse, the particles have time to change their position in the resonance domains under the action of the van der Waals attractive forces due to a decrease in the elasticity modulus of the heated adsorption layer of the particles. As a result, the particles in the resonant domains approach each other, and a decrease in the interparticle gaps results in a shift of the resonance of these domains to the long-wave range of the spectrum.[7,27]

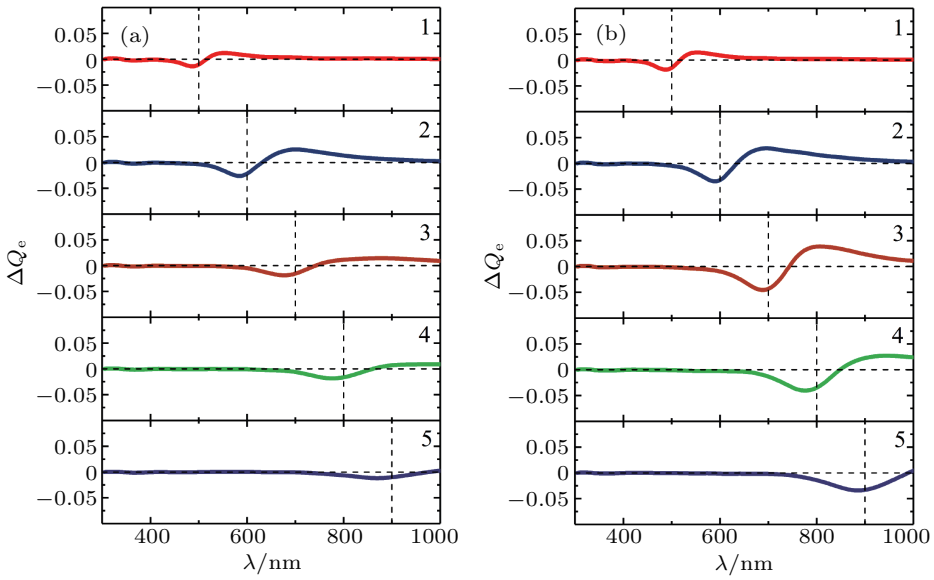

Fig. 5. Differential extinction spectra of multiparticle ($N = 50$) (a) monodisperse and (b) polydisperse aggregates of Ag nanoparticles at the moment of termination of a laser pulse with a duration of 20 ns and intensity 2.66×10^5 W·cm^{-2}. The vertical dotted line indicates the wavelength of the laser radiation.

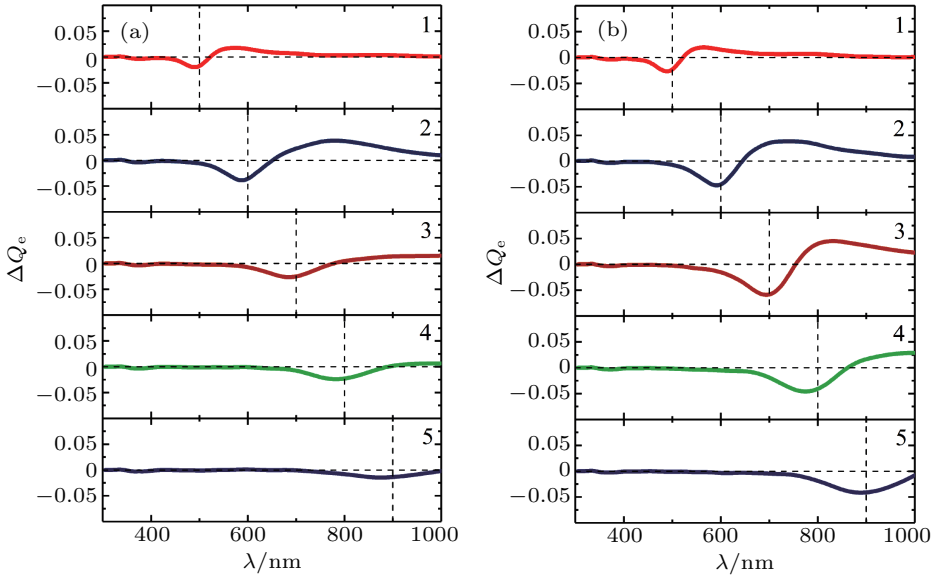

Fig. 6. Differential extinction spectra of multi-particle (a) monodisperse and (b) polydisperse aggregates of Ag nanoparticles 40 ns after the beginning of a pulse of 20 ns duration with an intensity of 2.66×10^5 W·cm^{-2}, the vertical dotted line indicates the laser wavelength.

An interesting feature of the nanosecond regime of photomodification is the pronounced asymmetry of the spectral dip with respect to the laser wavelength. This effect is observed in both monodisperse and polydisperse aggregates. Note that appearance of such a spectral feature can be responsible for the negative nonlinear refraction in an aqueous medium containing plasmonic multiparticle aggregates.[22,23] Figures 5 and 6 show a dip in the short-wave range in the differential absorption spectra. It is such position of a dip that a hump can cause a negative nonlinear refraction in nanosecond laser pulses.

In nanosecond pulses, particles in resonant domains have time to change their position during the pulse under the action of the van der Waals forces in conditions of a decrease in the elasticity modulus of the adsorption layer of the particles. At the same time, as a result of strong heating of particles, their resonant properties change. In this case, the domains with resonance frequency in the long-wave range of the spectrum coinciding with the laser radiation wavelength cease resonance interaction with the radiation and their particles stop heating. On the other hand, domains with resonance bands in the short-wave range change their resonant frequencies and approach to the laser radiation frequency, which results in greater heating of their particles. This combination of negative feedback for particles in the long-wavelength domains of aggregates and positive feedback for short-wave domains results in formation of strong asymmetry in the spectral dip. The presented results are consistent with experimental data obtained earlier.[21]

4. Conclusion

We have found the principal features of photochromic reactions in pulsed laser fields in plasmonic nanocolloids with aqueous environment containing disordered Ag nanoparticle aggregates. These features reproduce the experimentally observed extinction spectra of Ag colloids irradiated by pulsed lasers. It was found that there are both a dynamic mode of laser modification of such aggregates occurring during a laser pulse, and a static mode occurring after the pulse. It was shown that the mechanisms of laser modification of such aggregates depend on the laser pulse duration and can be associated both with changes in the resonant properties of the particles due to their heating and melting (picosecond irradiation mode), and with the particle shifts in the resonant domains of the aggregates (nanosecond pulses). Both of these mechanisms result in formation of a narrow asymmetric dip near the laser radiation wavelength in the plasmonic absorption spectrum of the aggregate and depend on the wavelength, intensity, polarization of the radiation as well as affect the shape and position of this dip in the spectrum. The static mode of laser modification occurs due to collapse of neighboring particles in the resonant domains of the aggregate, even after the pulse end. When exposed to long (nanosecond) pulses, the dip can insignificantly drift to the long-wavelength spectral range even after the pulse termination. When exposed to laser radiation on the resonant and quasi-resonant domains of the aggregate, the particles approach each other during the pulse. This means that the particles in domains with small (about 20–30 nm) short-wavelength spectral shift (relative to the laser radiation wavelength) may be in resonance with the radiation by the end of the pulse. In this case, the initial resonance domains will be out of the resonance and will have a long-wavelength shift relative to the radiation wavelength. This results in formation of a hump on the long-wavelength side of the dip in the differential spectrum. Herewith, the radiation affects the quasi-resonance domains in the long-wave side of the resonance, but their heating results in collapse of particles and an even greater long-wavelength shift of the resonances. Thus, these domains quickly cease the

resonant interaction with radiation.

References

[1] Schuck P J, Fromm D P, Sundaramurthy A, Kino G S and Moerner W E 2005 *Phys. Rev. Lett.* **94** 017402

[2] Kühn S, Håkanson U, Rogobete L and Sandoghdar V 2006 *Phys. Rev. Lett.* **97** 017402

[3] Carminati R, Greffet J J, Henkel C and Vigoureux J 2006 *Opt. Comm.* **261** 368

[4] Rogobete L, Schniepp H, Sandoghdar V and Henkel C 2003 *Opt. Lett.* **28** 1736

[5] Sun G and Khurgin J B 2011 *Plasmonics and Plasmonic Metamaterials* (Singapore: World Scientific) pp. 1–44

[6] Gavrilyuk A P and Karpov S V 2009 *Appl. Phys. B* **97** 163

[7] Ershov A E, Gavrilyuk A P, Karpov S V and Semina P N 2014 *Appl. Phys. B* **115** 547

[8] Ershov A E, Gerasimov V S, Gavrilyuk A P and Karpov S V 2017 *Appl. Phys. B* **123** 182

[9] Shalaev V M 1996 *Phys. Rep.* **272** 61

[10] Shalaev V M 2000 *Nonlinear optics of random media: fractal composites and metal dielectric films* (Berlin: Springer Verlag)

[11] Karpov S V and Slabko V V 2003 *Optical and photophysical properties of fractal-structured metal sols* (Novosibirsk: Russian Academy of Sciences, Siberian Branch)

[12] Pyatenko A, Wang H, Koshizaki N and Tsuji T 2013 *Laser & Photonics Reviews* **7** 596

[13] Liu X, Chen H, Chen X, Alfadhl Y, Yu J and Wen D 2014 *J. Appl. Phys.* **115** 094903

[14] Richardson H H, Carlson M T, Tandler P J, Hernandez P and Govorov A O 2009 *Nano Lett.* **9** 1139

[15] Xu B, Song R G, Wang C and He W Z 2012 *Materials Processing Technology II* (Stafa-Zurich: Trans Tech Publications Ltd) pp. 1888–1891

[16] Karpov S V, Gerasimov V S, Isaev I L and Markel V A 2005 *Phys. Rev. B* **72** 205425

[17] Karpov S V, Gerasimov V S, Isaev I L, Podavalova O P and Slabko V V 2007 *Colloid J.* **69** 159

[18] Karpov S V, Bas'ko A L, Popov A K and Slabko V V 2000 *Colloid J.* **62** 699

[19] Karpov S V, Popov A K, Rautian S G, Safonov V P, Slabko V V, Shalaev V M and Shtokman M I 1988 *JETP Lett.* **48** 571

[20] Safonov V P, Shalaev V M, Markel V A, Danilova Y E, Lepeshkin N N, Kim W, Rautian S G and Armstrong R L 1998 *Phys. Rev. Lett.* **80** 1102

[21] Karpov S V, Popov A K and Slabko V V 2003 *Technical Phys.* **48** 749

[22] Karpov S V, Kodirov M K, Ryasiyanskiy A I and Slabko V V 2001 *Quantum Electronics* **31** 904

[23] Ganeev R A, Ryasnyansky A I, Kamalov S R, Kodirov M K and Usmanov T J 2001 *Physica D* **34** 1602

[24] Gavrilyuk A P and Karpov S V 2010 *Appl. Phys. B* **102** 65

[25] Markel V A 1993 *J. Mod. Opt.* **40** 2281

[26] Ershov A E, Isaev I L, Semina P N, Markel V A and Karpov S V 2012 *Phys. Rev. B* **85** 045421

[27] Ershov A E, Gavrilyuk A P, Karpov S V and Semina P N 2015 *Chin. Phys. B* **24** 47804

[28] Drachev V P, Perminov S V, Rautian S G, Safonov V P and Khaliullin E N 2002 *J. Exp. Theor. Phys.* **94** 901

[29] Drachev V P, Perminov S V and Rautian S G 2007 *Opt. Express* **15** 8639

[30] Perminov S V, Drachev V P and Rautian S G 2008 *Opt. Lett.* **33** 2998

[31] Perminov S V and Drachev V P 2009 *Opt. Spectrosc.* **107** 987

[32] Rautian S G 2004 *Opt. Spectrosc.* **97** 416

[33] Gavrilyuk A P, Gerasimov V S, Ershov A E and Karpov S V 2018 *Colloid and Polymer Science* **296** 1689

[34] Mahanty J and Ninham B W 1976 *Dispersion Forces* (London-New York-San Francisco: Academic Press)

[35] Bargeman D and van Voorst Vader F 1972 *Journal of Electroanalytical Chemistry and Interfacial Electrochemistry* **37** 45

[36] Kreibig U and Vollmer M 1995 *Optical Properties of Metal Clusters* (Berlin: Springer-Verlag)

[37] Berry M V and Percival I C 1986 *Optica Acta* **33** 577

[38] Karpov S V, Gerasimov V S, Isaev I L and Obushchenko A V 2006 *Colloid J.* **68** 441